



Innovative ToF Sensors for Robotic Autonomous Systems

Azer Sadigov¹, Kenan Isayev², Jalal Naghiyev³

¹ *Innovation and Digital Development Agency, Baku, Azerbaijan,*
E-mail: azer.sadigov@idda.az

² *Innovation and Digital Development Agency, Baku, Azerbaijan,*
E-mail: kenan.isayev@idda.az

³ *Innovation and Digital Development Agency, Baku, Azerbaijan,*
E-mail: jalal.naghiyev@idda.az

Abstract. The paper presents the comprehensive results of an in-depth study focused on the latest advancements in silicon-based avalanche sensors. Detailed descriptions of the designs of various experimental samples are provided, highlighting their distinctive features and making thorough comparisons with analogous devices currently available on the market. The paper delves into the challenges associated with existing avalanche devices, exploring the underlying reasons that limit their operational parameters. Through rigorous analysis, it was determined that the sensors under investigation demonstrate superior performance compared to their counterparts, particularly in terms of photon registration efficiency and geometric factor. Furthermore, the paper introduces an innovative design aimed at addressing and resolving the performance issues commonly encountered in conventional sensors. This new design not only enhances the overall functionality of the sensors but also expands their potential applications. The study identifies several areas where this unique sensor design can be effectively utilized, particularly in international scientific projects. By providing a detailed exploration of these applications, the paper underscores the significant impact and potential of the new silicon-based avalanche sensors in advancing scientific research and technological development on a global scale.

Keywords: Sensor, SiPM, Silicon photomultiplier, Lidar, Time of Flight, ToF.

1. Introduction

Time-of-flight (also known as Time-of-Flight or TOF) refers to measurement techniques based on measuring the time it takes particles, waves or impulses to travel a certain distance. These methods are widely used in various fields of science and technology, which are based on the principle of transit time measurement, which allows the determination of various parameters with high accuracy and their application in a wide range of scientific and industrial applications.

Silicon avalanche photodiodes (SiPM) as sensors are key components for Time-of-Flight (TOF) [1] measurements in a variety of scientific and engineering applications. These devices use the principle of avalanche multiplication to detect photons with high sensitivity and accuracy. In this context, silicon avalanche photodiodes offer several advantages and capabilities, such as high sensitivity and fast response, which allows efficient detection of weak light signals. This is especially important in TOF systems, where accurate measurement of photon arrival times is critical. The high response speed of these diodes allows for highly accurate time-of-flight measurements, which improves spatial resolution and measurement accuracy. Low noise level, which improves data quality and reduces measurement errors. The small size and ability to integrate silicon avalanche photodiodes with other electronic components make them convenient for use in portable and compact automation systems.

Silicon avalanche photodiodes for time-of-flight measurements are an important element of modern scientific and engineering systems. Their high sensitivity, speed and low noise levels make them indispensable in applications requiring high precision and reliability. Continued research and development in this area is helping to improve the performance of these devices and expand their application into new fields of science and technology.

Leading manufacturers and research centers provide various designs of avalanche photodetectors tailored for different applications. These photodetectors, often referred to as photodiodes, are

predominantly available in two main configurations: surface pixel and internal pixel structures. Both types feature individual micropixels that incorporate a passive element, such as microresistors or microcapacitors, on a shared substrate. Each photodiode pixel operates in Geiger mode, possessing unique photoelectronic recording capabilities. Separate passive pixels are utilized to halt the avalanche process, and the parallel connection of these micropixels ensures the photodetector's linearity.

An Azerbaijani scientist, Z. Sadygov [2], was the pioneer who first proposed silicon photomultipliers (SiPMs) and patented their basic designs. Over the past decade, various modifications of Microcell Avalanche Photodiode (MAPD) photodetectors have been investigated. The initial structure features independent p-n junctions (micropixels) and is known commercially as a silicon photomultiplier or micropixel photo counter (MPPC). A limitation of this design is the restricted linear amplitude range, attributed to the low pixel density resulting from the arrangement of pixels and microresistors on the photodiode's surface. Increasing the pixel density beyond 1000 pixels/mm² significantly reduces the photodetector's sensitive area, consequently impairing photon detection efficiency and amplitude resolution. Currently, a primary research focus is on enhancing photon detection efficiency, resolution, speed linearity (recovery time), and amplitude of avalanche photodiodes.

2. Structures

The new structure of the MAPD photodiode is depicted in Figure 1 this structure called MAPD with buried pixels [3]. It comprises an n-type substrate serving as a base, with two epitaxial layers grown on top. Between these layers, there is an array of highly doped n++ pixels. The photodiode measures 3.7 × 3.7 mm² in area, with a pixel pitch of 15 μm and a pixel diameter of 12 μm, resulting in a pixel density of 4450 pixels/mm². The total number of pixels in the MAPD is 61000. The first epitaxial layer is 6 μm thick, and the second is 3 μm thick. To reduce the operational voltage of the MAPD, the specific resistance of these layers is tailored to 20 Ω × cm and 3 Ω × cm, respectively. The photodiode operates at approximately 55.6V.

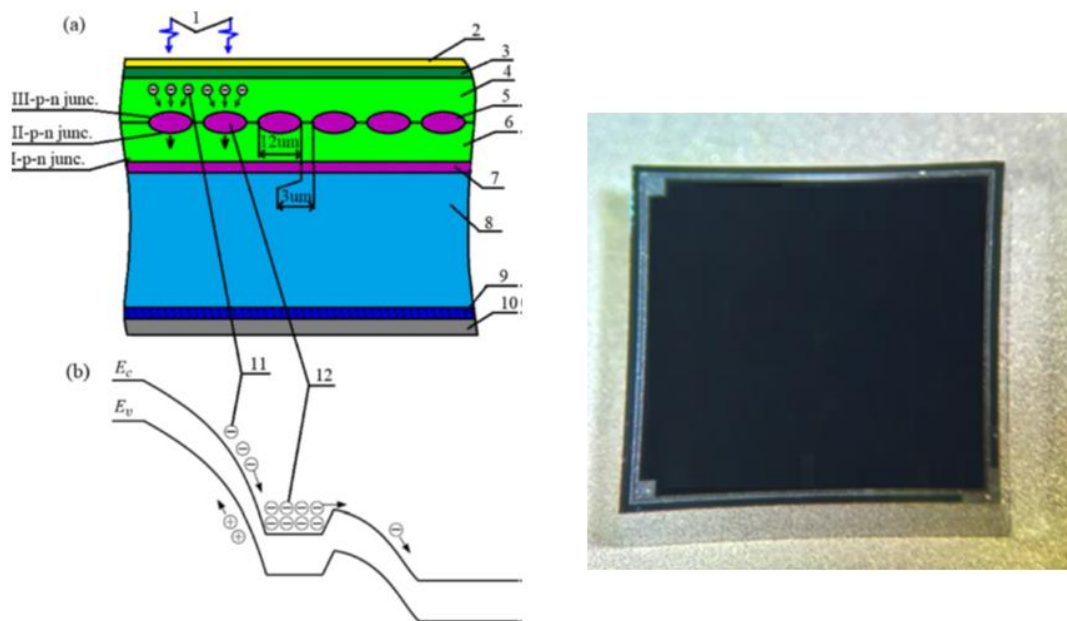


Figure 1. Schematic view of the photodetector concept (left) and experimental sample (right). Schematic diagrams showing the transverse section (a) and the energy band diagram (b) of the MAPD. Key components are labeled as follows: (1) incident photons; (2) SiO₂ layer; (3) highly doped p+ layer facilitating contact with the p-type epitaxial layer; (4) second p-type epitaxial layer; (5) n+ regions representing the micropixels; (6) first p-type epitaxial layer; (7) highly doped n+ layer defining the boundaries of the depletion region; (8) n-type silicon substrate; (9) highly doped n+ layer

ensuring contact with aluminum; (10) aluminum contact; (11) avalanche region; (12) charge accumulated in the potential well of the n+ micropixel.

This design stands out as unique due to the imaginary damping resistance generated when a reverse bias is applied. This characteristic enables the pixel density to be increased significantly, reaching up to 40,000 pixels per square mm. Such an exceptionally high pixel density ensures that the entire surface of the device becomes active, which in turn boosts the efficiency of photon registration by 25% when compared to surface-pixel analogues. Additionally, this design operates effectively at low light frequencies, further enhancing its performance and making it highly advantageous for applications requiring precise photon detection and high sensitivity.

To enhance the speed of the TOF sensor, it was determined that a fundamentally new avalanche photodetector was needed [4]. The issue lies in the high specific capacitance of MAPD photodetectors, which ranges from 10 to 50 pF/mm² due to their semiconductor nature. This high capacitance limits the device's performance as its sensitive area increases. The micropixel avalanche phototransistor (MAPT) addresses this problem effectively. The MAPT incorporates a matrix of micropixels, each with its own quenching resistor, similar to the traditional MAPD. Additionally, it includes a matrix of microtransistors, each with individual ballast resistors. The micropixels are connected through quenching resistors to a common metal conductor, while the microtransistors are connected through ballast resistors to a separate metal conductor. Consequently, the device features two independent signal outputs: a "pixel output" linked to the micropixel circuit and a "transistor output" connected to the microtransistor circuit (refer to Fig. 2).

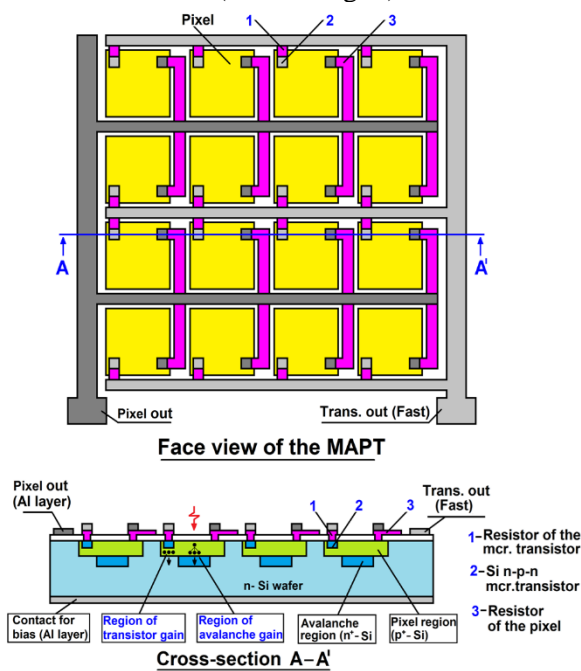


Figure2. Design of a micropixel avalanche phototransistor (left) and photo (right). 1- Micropixel, 2-Micropixel Resistor, 3-Microtransistor, 4-Microtransistor Resistor.

The MAPT principle of operation is based on the specifics of the MAPD pixel operation in the Geiger mode (in the overvoltage mode). The avalanche process in the pixel causes a voltage drop there greater than 0.75V, which is enough to completely open the emitter-base (or pixel) junction of the microtransistor, and as a result of this, a current flows through the microtransistor's electrical circuit, limited only by its ballast resistor. The microtransistor closes when the potential of the base (pixel) relative to the emitter drops below 0.75V, due to the discharge of the micropixel capacitance. A microtransistor is formed directly over a small portion of the pixel area. The microtransistor has a size of 4 μ *4 μ which occupies about 3% of the area of a 25 μ *25 μ micropixel. In this case, the specific capacitance of the microtransistor will be 80 times less than the corresponding capacitance of the pixel,

which is equivalent to a decrease in the effective capacitance of the device, since the signal is taken from the microtransistor circuit. For example, if the overvoltage is 1V, the maximum potential change per pixel is 2V. It can be calculated that the photocurrent J_p in the pixel circuit leads the current $J(tr.)$ in the microtransistor circuit, since the beginning and end of the latter is determined by the potential at the pixel (ie, the potential at the base). The microtransistor opens at the time t , when the avalanche process has time to discharge the pixel by $\Delta U_{dp} = U_d - U_p(t) = 0.75V$. Thus, the photocurrent J_p in the pixel circuit and the current $J(tr.)$ in the microtransistor circuit can be described by the expressions

$$J_p = \frac{\Delta U_{dp}}{R_q}, \quad J_{tr.} = \frac{\Delta U_{dp}^{-0,75}}{R_{tr.}}$$

where $U_{dp} = U_d - U_p(t)$ is the potential change at the pixel, U_d is the external voltage applied to the MAPT, $U_p(t)$ is the current potential at the pixel.

Methods for picking up a fast signal from MAPD (or SiPM) pixels using an independent electrode are known in the scientific literature. For example, special microcapacitors formed on a part of the pixel surface are used for this. All micro-capacitors are connected to an additional metal bus, which has an independent output for removing the fast signal ("fast out").

3. Performance of MAPD

The PDE coefficient was determined. The reference sample photodiode from well known manufacturer Hamamatsu MPPC S13360-3025, which PDE is known (25%), was placed in the black box shown in Figure 3. The sample was illuminated by a light diode with a wavelength of 450 nm, to which a 30 ns pulse was applied from a generator with a frequency 50 kHz and an amplitude of 2.92 V. One of the methods outlined earlier was to find the breakdown voltage for a given temperature (in our case, the temperature was $-6^\circ C$). It is known that for these photodiodes the operating voltage is determined as follows:

$$U_{op} = U_{br} + 5V \quad (1)$$

At this temperature, U_{br} turned out to be equal to 50.08 V. By changing the voltage within five volts, we obtain the operating voltage. Using a single-photoelectron spectrum, the number of registered events was determined and the average number of registered photons in one pulse μ was found through formula (2).

$$\mu = -\ln\left(\frac{N_{tot} - N_{det}}{N_{det}}\right) \quad (2)$$

where N_{tot} is the total number of events for these LED parameters that occurred in three minutes ($N_{tot} = F \cdot t = 50 \cdot 10^6 \cdot 180 = 9 \cdot 10^6$ counts), N_{det} is the number of registered events.

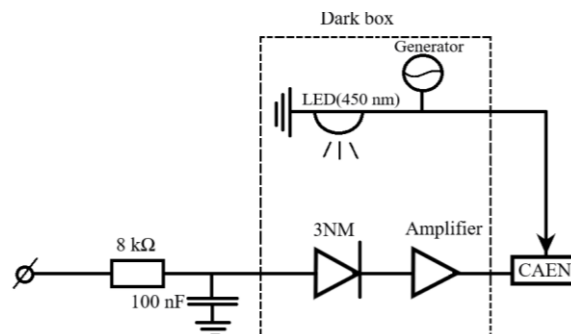


Figure 3. Experimental setup

At an operating voltage of 55.08 V, the average number of recorded photons in one pulse μ equal to $1.33 \cdot 10^6$ was obtained. From formula

$$PDE = \frac{\mu}{N_{ph}} \quad (3)$$

using a simple relationship, you can find the number of photons, knowing the PDE for Hamamatsu S13360-3025 photodiodes. Their number was found to be $5.3 \cdot 10^6$. However, these photodiodes have an area of 3x3 mm, and the MAPD, which PDE will be measured next, have an area of 3.7x3.7 mm. From a simple relationship, it was found that for MAPD photodiodes the number of photons is $8.06 \cdot 10^6$.

The reference photodiode was replaced with a MAPD and cooled to the same temperature of -6 °C. Its breakdown voltage $U_{br} = 51.2$ V was determined, as well as its operating voltage in the manner described above. Next, for various operating voltages, the average number of recorded photons in one pulse was found. PDE was determined through formula (3). Table 1 below shows the research results.

U, V	$\mu \cdot 10^6$, counts	PDE, %
53,7	2,16	29,7
54,2	2,25	30,9
54,7	2,4	32,8

4. Performance of MAPT

The experimental data depicted in Figure 4 demonstrate a notable advantage of the micropixel avalanche phototransistor over the SiPM from well-known manufacturer SensL. The comparison between these two devices was conducted by applying appropriate bias voltages to each, achieving a gain of approximately $M \approx 1.5 \cdot 10^6$ in both. The red curve represents the photosignal from the transistor output of our photodiode with transistor amplification, while the blue curve indicates the photosignal from the capacitive (or fast) output of SensL's photodiode. Both signals were amplified using identical amplifiers with an 80 MHz bandwidth and a gain of 100, and then fed to an oscilloscope with a 200 MHz bandwidth. Although the signal edges were determined by the amplifier's bandwidth, this did not affect the accuracy of the comparison.

The signal amplitude from the fast output of our developed MAPT can be significantly enhanced by increasing the overvoltage and decreasing the resistance of the ballast resistor $R_{(tr.)}$. This adjustment will notably increase the growth rate (mV/ns) of the signal's leading edge, thereby improving the timing accuracy in TOF systems.

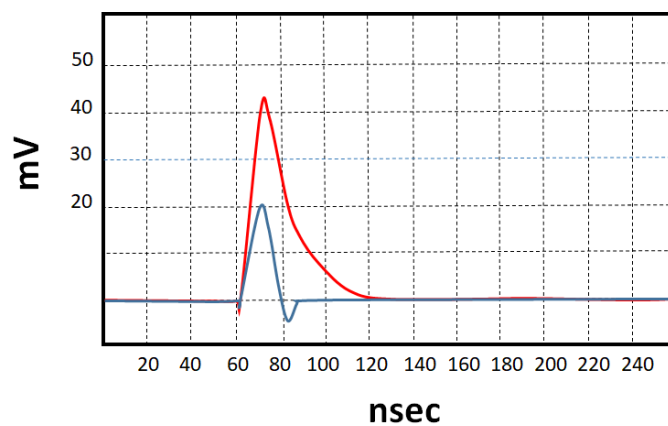


Figure 4. Oscillogram of photodiodes. The red curve is the photo signal from the MAPT, the blue curve is the photo signal of the photodiode from the SensL company

4. Acknowledgment

This work has partly received funding from the European Union's Horizon 2022 Research and Innovation Programme under the Marie Skłodowska-Curie's DETMED project (grant agreement ID 101129879).

5. Conclusion

New designs of avalanche sensors are presented. It was revealed that MAPD has better photon registration performance than known analogues. It was revealed that the signal received from the fast output of the MAPD is 2 times higher than the signal received from known analogues.

References

1. Chung, C.; Backes, T.; Dittmar, C.; Karpinski, W.; Kim, T.; Louis, D.; Schwering, G.; Wloch, M.; Schael, S. The Development of SiPM-Based Fast Time-of-Flight Detector for the AMS-100 Experiment in Space. *Instruments* 2022, 6, 14. <https://doi.org/10.3390/instruments6010014>
2. Sadygov Z., Sadigov A., Khorev S. Silicon photomultipliers: Status and prospects // *Physics of Particles and Nuclei Letters*. – 2020. – T. 17. – C. 160-176. <https://doi.org/10.1134/S154747712002017X>
3. Ahmadov F. et al. Investigation of parameters of new MAPD-3NM silicon photomultipliers // *Journal of Instrumentation*. – 2022. – T. 17. – №. 01. – C. C01001, <https://doi.org/10.1088/1748-0221/17/01/C01001>
4. Sadigov A. et al. A new detector concept for silicon photomultipliers // *Nuclear Instruments and Methods in Physics Research Section A: Accelerators, Spectrometers, Detectors and Associated Equipment*. – 2016. – T. 824. – C. 135-136. <https://doi.org/10.1016/j.nima.2015.11.013>